Contributions, Geophysical Institute, Kyoto University, No. 13, 1973, 13–20

SCHUMANN RESONANCE FREQUENCIES AND THE CONDUCTIVITY PROFILES IN THE ATMOSPHERE

By

Toshio OGAWA and Yutaka MURAKAMI

(Received August 31, 1973)

Abstract

An automatic tracker of Schumann resonances was made and the vertical electric component was measured with a ball antenna. Average peak frequencies of each month from October 1971 to April 1972 were obtained. Overall average frequencies are 7.65, 14.12 and 20.35 Hz for the first three modes respectively. These frequencies agree very well with the previous observations in 1967–1968. On the other hand resonance frequencies from multi-signal sources are calculated with the atmospheric and lower ionospheric conductivity profiles from 10 to 140 km. Relatively good agreement between the experimental and theoretical resonance frequencies is obtained showing that the present conductivity profiles based on the balloon and rocket observations in mid-latitudes are better approximations of the world-wide average conductivity models for Schumann resonances than those in previous works.

1. Introduction

The electromagnetic resonance phenomena in the cavity between the earth and the ionosphere were first studied by Schumann [1952a, b] and they are called Schumann resonances which attract much interest in the fields of geophysics as well as of radio propagation.

Schumann resonances are related to the worldwide thunderstorm distributions which are considered as main signal sources, and the conductivity profiles in the atmosphere as well as in the lower ionosphere, both of which make an upper boundary of the cavity in the global scale. As the actual earth-ionosphere cavity has a very low Q factor, most of electromagnetic energy is dissipated within the upper boundary. The absolute values of resonance frequencies, therefore, are mainly determined by the atmospheric and lower ionospheric conductivity profiles.

The diurnal patterns of the resonance frequencies are mainly controlled by the diurnal variation of the worldwide thunderstorm distributions which are considered main signal sources. As the thunderstorm distributions at the designated times in a day are not thought to change very much day by day during a relatively short period, say a month, the observed fluctuations from the mean values of the resonance frequencies mainly depend on the perturbations of lower ionospheric conductivity profile by solar activity.

Our main purposes of studies of Schumann resonances are to clarify the above

three geophysical causes and effects, that is the relations between (1) the resonance frequencies and the atmospheric and lower ionospheric conductivity profiles, (2) the diurnal patterns of the resonance frequencies and the worldwide thunderstorm distributions in terms of space and time, and (3) the fluctuations of the resonance frequencies and the solar activity. In this paper we present one of the results of the relations between the resonance frequencies and the atmospheric and lower ionospheric conductivity profiles.

2. Observations

An automatic resonance tracking system of Schumann resonances was made referring to Nelson [1967]. It contains an automatic variable tuning circuit which follows to the maximum point of spectral density of received signals. The natural electromagnetic noises in the frequency band of the lowest ELF are received with a ball antenna which is placed on the roof of the building of the Geophysical Institute and are fed to an amplifilter of the frequency band of 5–30 Hz with the gain of 60 db at the flat portion and of −60 db at 60 Hz, the commercial power line frequency. The signals through the amplifilter are fed to the tracker.

The frequency bands of tracking filters are 7.8 ± 1.5 Hz, 14.0 ± 1.5 Hz and 20.0 ± 1.5 Hz for the first three resonance modes respectively. The attenuation of the filters of each modes is over −12 db/oct. The AGC characteristic in the input is that an input change of 10 db corresponds to within an output change of 0.5 db. The output voltages of frequency monitor are 0–1 volt corresponding to the respective filter band ranges. The block diagram of whole observing system is shown in Fig. 1. Q factors and amplitudes of resonances are also monitored as shown in Fig. 1.

The frequency calibration is made in the following way. A radiator antenna was

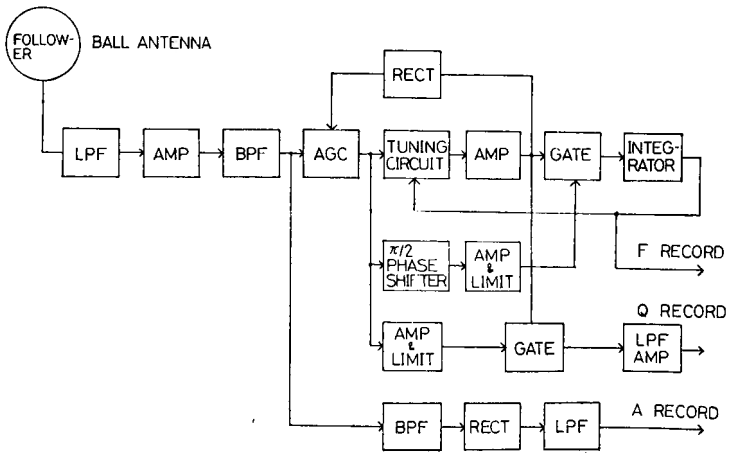

Fig. 1. Observing system of Schumann resonances. The automatic tracker connected to the ball antenna is shown.

placed a few meters—a fixed distance—apart from the receiving ball antenna. The output of an ultralow frequency oscillator is connected to this radiator antenna. The frequency and the amplitude of the signals from the oscillator are calibrated with the frequency counter and the AC voltmeter. The ball antenna receives the radiated signals at fixed frequencies in the Schumann resonance frequency range. The frequency accuracy is thus improved to ± 0.02 Hz from ± 0.13 Hz which was the accuracy in the case using a sonagraph (Ogawa et al., [1968]).

3. Observed resonance frequencies

Data during 7 months from October 1971 to March 1972 were analyzed. Peak frequencies were read every hour and were averaged every month for the first three modes. In the processes of data statistics are omitted the portions apparently disturbed by severe weather or artificial noises. Monthly mean resonance frequencies are listed in Table 1, in which overall average frequencies are also obtained as 7.65, 14.12 and 20.35 Hz for the fundamental, second and third modes respectively. These values are in good agreement with the values 7.69, 14.1 and 20.3 Hz obtained before by using the sonagraph from the data in 1967-1968 (Ogawa et al., [1968]). It is concluded from these experimental results that the average atmospheric and lower ionospheric conductivity distributions were not essentially changed over these five years.

4. Computational Method

The Schumann resonance phenomena have been extensively studied by Jones [1967, 1969], and Jones and Kemp [1970] using the single-source model. In this paper a multi-source model is developed. In the present stage of theory, the following two simplifications will be made, following the method of Jones [1967] and Jones and Kemp [1970]. (1) The terrestrial ionosphere is assumed to be spherically stratified; that is, the difference of the distribution of electrical conductivity between the day and night hemispheres is not taken into account. (2) The terrestrial magnetic field is assumed to have only a slight effect upon the phenomena. Under these assumptions, the vertical component of the electric field, radiated from a vertical electric dipole oscillating at the angular frequency ω, can be evaluated by the equation

$$E_r(\omega, \nu, \theta) = \frac{[Il](\omega)\nu(\nu+1)}{4\pi a^2 i\varepsilon_0 \omega h} \sum_{m=0}^{\infty} \frac{(2m+1)P_m(\cos\theta)}{m(m+1)-\nu(\nu+1)}, \tag{1}$$

Table 1. Observed average Schumann resonance frequencies (Hz)

	1971			1972				
Mode	Oct.	Nov.	Dec.	Jan.	Feb.	Mar.	Apr.	Mean
1	7.64	7.71	7.70	7.64	7.66	7.62	7.58	7.65
2	14.05	14.12	14.19	14.24	14.11	14.06	14.08	14.12
3	20.33	20.27	20.23	20.33	20.35	20.43	20.52	20.35

where $\nu(\nu+1)=k^2a^2(1-C^2)$, and $R_gR_i\exp(-i2khC)=1$. The notation is the same as in Jones [1967], and Jones and Kemp [1970]. The reflection coefficient R_i of the ionosphere is calculated following the method of Wait, which is fully described in Jones [1967]. In the present calculations the height h of the conducting layer is taken to be 10 km, and the layer is divided into 80 or 85 layers between 10 km and 140 km.

Three conductivity profiles used in the calculations are shown in Fig. 2. The three profiles are the same in the region above 60 km. The profile C below 90 km is that of Cole and Pierce [1965], above which the conductivity is computed from the electron density profile arranged by Maeda [1969] from the rocket experiments in mid-latitude and the collision frequency profile by Nicolet [1953]. Below 60 km in the profile (A) our own measurements by balloons in 1968 and 1969, which will be published elsewhere, are used in the region from 10 to 30 km. The profile between 30 and 60 km is extrapolated from both up- and down-profiles. In the profile (B), the conductivity at 10 km is made twice as much as that of profile (A) in order to imitate the "average" profile very recently reviewed by Hake et al. [1973].

As signal sources are more than one, the electric field computed by Eq. (1) must be added up in a certain manner. For convenience sake the earth's surface was divided into 24 zones by 23 equi-angular contours at intervals every 7.5 degrees from the observer. N_i being the number of dipoles in the i-th zone from the observer, the intensity of electric vertical component radiated from $\sum_{i=1}^{24}N_i$ sources all over the world may be evaluated from the equation

$$|E(\omega,\nu)|=\sqrt{\sum_{i=1}^{24}N_i|E_r(\omega,\nu,\theta_i)|^2}\,. \tag{2}$$

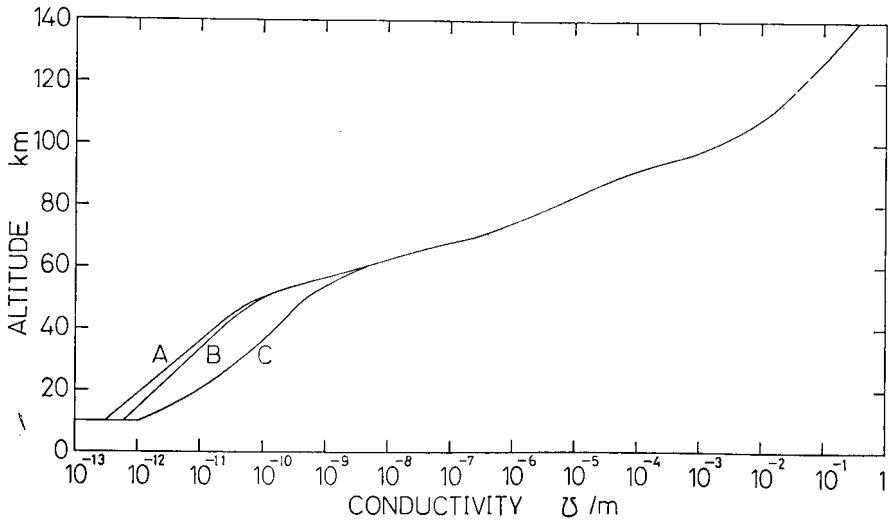

Fig. 2. Conductivity profiles used for the calculations. For A, B and C, see text.

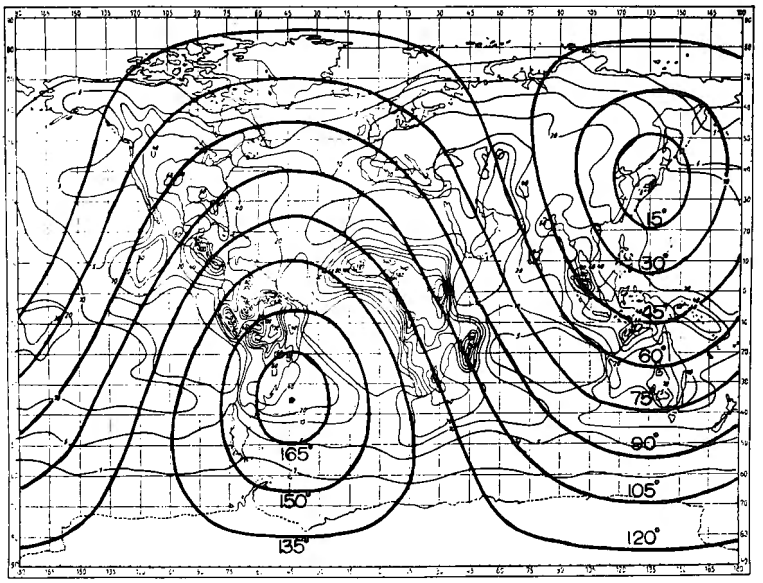

Fig. 3. Map of geographical distribution of average annual numbers of thunderstorm days. Equiangular contours from Kyoto are shown every 15°.

The electric field can be calculated for various ω's, and then the ω's which give the maximum value of the field can be found. These are peak frequencies.

Fig. 3 is a map of the geographical distribution of average annual numbers of thunderstorm days (Israël [1961]), upon which are drawn equi-angular contours from Kyoto every 15 degrees. This map is assumed to represent the distribution of average diurnal numbers of lightning discharges. The earth's surface is again divided into 24 columns by longitudinal lines in Fig. 3. If N_{ij} lightning discharges occur during an average day in a region where the i-th zone from the observer and the j-th column from the left overlap each other, and $M_k\%$ of N_{ij} lightning discharges are active at k hours LT, the numbers of lightning discharges which are active at T hours UT all over the i-th zone can be found from the equation

$$N_i(T)=\frac{1}{100}\sum_{j=1}^{24}N_{ij}M_{T+j-13}. \tag{3}$$

From Eqs.(1), (2) and (3), peak frequencies at T hours UT can be found.

The local time dependency of M_k is listed in Table 2. Different values over land and oceans are adopted. The diurnal variation of local thunderstorm activities over land is based upon the data of Maxwell and Stone [1966] (refer to Galejs [1972]), and those on oceans are assumed to be constant. From the space and time distributions of thunderstorm activity in Fig. 3 and Table 2 is calculated the diurnal variation of relative source activity which is shown in Fig. 4. This is very similar to the diurnal variation of the potential gradient observed on oceans which is considered as a global

Table 2. Diurnal variation of lightning activity (M%)

Local time	0	1	2	3	4	5	6	7	8	9	10	11
Land	3.2	2.5	2.3	2.3	2.3	2.1	1.8	1.6	1.7	1.9	2.4	2.9
Ocean	4.2	4.2	4.2	4.2	4.2	4.2	4.2	4.2	4.2	4.2	4.2	4.2
Local time	12	13	14	15	16	17	18	19	20	21	22	23
Land	3.9	5.0	6.3	7.0	7.3	7.4	7.2	7.0	6.5	6.0	5.2	4.4
Ocean	4.2	4.2	4.2	4.2	4.2	4.2	4.2	4.2	4.2	4.2	4.2	4.2

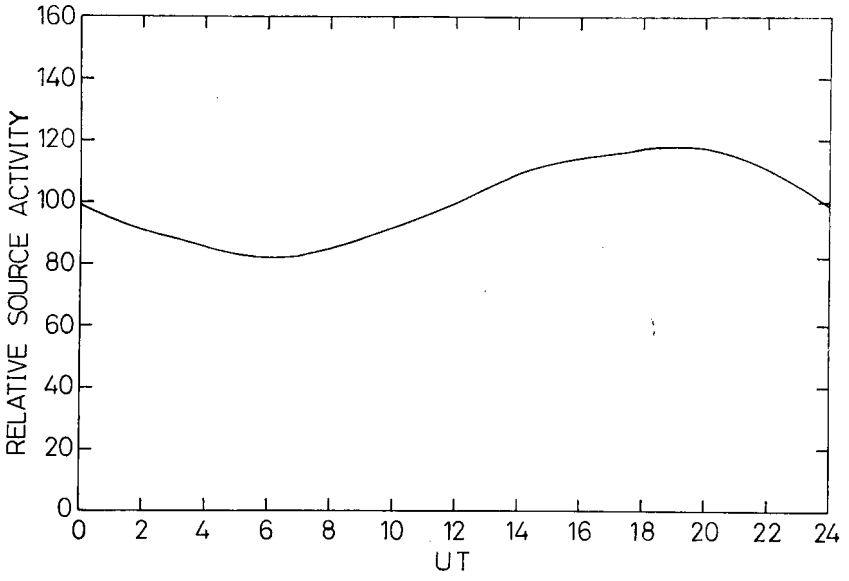

Fig. 4. Diurnal variation of relative signal source activity.

effect of thunderstorm electricity.

According to the method mentioned above, values and variations of Schumann resonance phenomena at any observing site can be calculated.

5. Computational results

Calculations were carried out for the three atmospheric and ionospheric profiles. Peak frequencies from the multi-signal sources were computed for the first three resonance modes every hour for a day. The calculated average peak frequencies for 24 hours and the ionospheric parameters at 8 Hz are shown together with the experimental results in Table 3. Ionospheric attenuation constant α and phase velocity v were calculated by the following equations. $\alpha=-0.182 f\cdot\mathrm{Im}(S)\mathrm{db/Mm}$, and $c/v=\mathrm{Re}(S)$, where $S=(1-C^2)^{1/2}$.

Relatively good agreements with the experimental results are found for the profiles A and B, although they give 3.8% larger values for the first mode and 1.0% smaller

Table 3. Calculated Schumann resonance frequencies (Hz) and ionospheric parameters

Conductivity profile	m-Resonator mode order			Ionospheric parameters at 8 Hz		
	1	2	3	α	c/v	Ω
A	7.94	14.11	20.16	0.1348	1.326	3.51
B	7.94	14.11	20.16	0.1414	1.326	3.69
C	7.45	13.67	19.63	0.2762	1.397	6.83
Observation	7.65	14.12	20.35			4.96

α: attenuation constant (db/Mm)

$\frac{c}{v}$: $\frac{\text{light velocity}}{\text{phase velocity}}$

Ω: damping coefficient (sec^{-1})

values for the third mode than observed values. The difference of conductivity profiles between A and B does not give any appreciable effect in all aspects.

A waveform of the electric vertical field excited by a dipole source of step function is given approximately by $e^{-\Omega t}\cos\omega t$. The damping coefficient Ω can be calculated by the following equation. $\Omega=\alpha(\text{m}^{-1})v(\text{m sec}^{-1})=34.54\times\alpha(\text{db/Mm})/c/v$, or $\alpha=8.686\times10^{6}\Omega/v$ (In the paper by Handa et al. [1971], 4.343 was misprinted in page 14 instead of 8.686). The average damping coefficient of Q type bursts for the electric vertical component was found to be 4.96 sec^{-1} by Handa et al. [1971]. Though the mechanism of Q-type bursts is not well known, it is certain that the damping coefficient has a close relationship to the atmospheric and ionospheric characteristics. Table 3 shows that the observed Ω is just between those calculated for profiles A and B and that for profile C.

The present method of calculation has an advantage of being able to calculate diurnal variations of resonance peak frequencies. The observed peak frequencies vary in certain diurnal variation patterns whose amplitudes are about 0.15, 0.25 and 0.30 Hz for the first, second and third modes respectively, and the numerical values given in Table 1 are their arithmetical averages, so the calculations should also explain the variation patterns of peak frequencies. But using the diurnal variation of lightning activity listed in Table 2, no appreciable variation in peak frequencies could be obtained. This means either that the diurnal variation of local lightning activity is more drastic, or that the diurnal variation of peak frequencies is caused by some reasons other than the variation of worldwide lightning activity. A computation which is not presented here showed that a more drastic diurnal variation of local lightning activity can explain the observed variation amplitude of peak frequencies. Diurnal variations of resonance peak frequencies will be discussed in the near future.

In conclusion the observed Schumann resonance frequencies are satisfactorily simulated at the present stage of investigation by calculations with more realistic atmospheric and ionospheric conductivity profiles A and B and worldwide multi-signal sources, most of which are based on the experimental data.

References

Cole, R. K., Jr. and E. T. Pierce, 1965; Electrification in the earth's atmosphere for altitudes between 0 and 100 kilometers, J. Geophys. Res., **70**, 2735–2749.

Galejs, J., 1972; *Terrestrial Propagation of Long Electromagnetic Waves,* Pergamon Press, Oxford, 362 pp.

Hake, R. D., Jr., E. T. Pierce and W. Viezee, 1973; Stratospheric electricity, Final report, Contract No. N00014-72-C-0259, SRI Project 1724, S. R. I., Menlo Park, Calif., 140 pp.

Handa, S., T. Ogawa and M. Yasuhara, 1971; Damping coefficients of Q-type bursts in the Schumann resonance frequency range, Contributions, Geophys. Inst., Kyoto Univ., No. **11**, 11–15.

Israël, H., 1961; *Atmosphärische Elektrizität, Teil II,* Akademische Verlagsgesellschaft, Leipzig, 503 pp.

Jones, D. L., 1967; Schumann resonances and e.l.f. propagation for inhomogeneous, isotropic ionosphere profiles, J. Atmosph. Terr. Phys., **29**, 1037–1044.

————, 1969; The apparent resonance frequencies of the earth-ionosphere cavity when excited by a single dipole source, J. Geomag. Geoelectr., **21**, 679–684.

———— and D. T. Kemp, 1970; Experimental and theoretical observations on the transient excitation of Schumann resonances, J. Atmosph. Terr. Phys., **32**, 1095–1108.

Maeda, K., 1969; Mid-latitude electron density profile as revealed by rocket experiments, J. Geomag. Geoelectr., **21**, 557–567.

Maxwell, E. L. and D. L. Stone, 1966; V.L.F. atmospheric noise predictions, Rep. 92-F-1, Contract No. 93159, DECO Electronics, Inc., Boulder, Colorado.

Nelson, P. H., 1967; Ionospheric perturbations and Schumann resonance data, PhD thesis, MIT., 109 pp.

Nicolet, M., 1953; The collisional frequency of electrons in the ionosphere, J. Atmosph. Terr. Phys., **3**, 200–211.

Ogawa, T., Y. Tanaka and M. Yasuhara, 1968; Diurnal variations of resonant frequencies in the earth-ionosphere cavity, Special Contributions, Geophys. Inst., Kyoto Univ., No. **8**, 15–20.

Schumann, W. O., 1952 a; Über die strahlungslosen Eigen-schwingungen einer leitenden Kugel, die von einer Luftschicht und einer Ionospharenhulle ungeben ist, Z. Naturforsch., **7A**, 149–154.

————, 1952 b; Über die Dampfung der elektromagnetischen Eigenschwingungen des Systems Erde-Luft-Ionosphare, Z. Naturforsch., **7A**, 250–252.